Bioorganic & Medicinal Chemistry Letters 20 (2010) 6258–6261

Contents lists available at ScienceDirect

Bioorganic & Medicinal Chemistry Letters

journal homepage: www.elsevier.com/locate/bmcl

Peripheral but crucial: A hydrophobic pocket (Tyr^{706}, Leu^{337}, and Met^{336}) for potent and selective inhibition of neuronal nitric oxide synthase

Fengtian Xue [a,†], Huiying Li [b], Jianguo Fang [a], Linda J. Roman [c], Pavel Martásek [c,‡], Thomas L. Poulos [b,*], Richard B. Silverman [a,*]

[a] Departments of Chemistry and Biochemistry, Molecular Biology, and Cell Biology, Center for Molecular Innovation and Drug Discovery, and Chemistry of Life Processes Institute, Northwestern University, 2145 Sheridan Road, Evanston, IL 60208-3113, USA
[b] Departments of Molecular Biology and Biochemistry, Pharmaceutical Chemistry, and Chemistry, University of California, Irvine, CA 92697-3900, USA
[c] Department of Biochemistry, The University of Texas Health Science Center, San Antonio, TX 78384-7760, USA

ARTICLE INFO

Article history:
Received 2 July 2010
Revised 17 August 2010
Accepted 18 August 2010
Available online 26 August 2010

Keywords:
Nitric oxide synthase
Selective inhibitor
Crystal structure
Peripheral hydrophobic pocket
Pi-stacking

ABSTRACT

Selective inhibition of the neuronal isoform of nitric oxide synthase (nNOS) over endothelial nitric oxide synthase (eNOS) and inducible nitric oxide synthase (iNOS) has become a promising strategy for the discovery of new therapeutic agents for neurodegenerative diseases. However, because of the high sequence homology of different isozymes in the substrate binding pocket, developing inhibitors with both potency and excellent isoform selectivity remains a challenging problem. Herein, we report the evaluation of a recently discovered peripheral hydrophobic pocket (Tyr^{706}, Leu^{337}, and Met^{336}) that opens up upon inhibitor binding and its potential in designing potent and selective nNOS inhibitors using three compounds, **2a**, **2b**, and **3**. Crystal structure results show that inhibitors **2a** and **3** adopted the same binding mode as lead compound **1**. We also found that hydrophobic interactions between the 4-methyl group of the aminopyridine ring of these compounds with the side chain of Met^{336}, as well as the π–π stacking interaction between the pyridinyl motif and the side chain of Tyr^{706} are important for the high potency and selectivity of these nNOS inhibitors.

© 2010 Elsevier Ltd. All rights reserved.

Overproduction of the small molecule nitric oxide (NO) by the neuronal isoform of nitric oxide synthase (NOS) in the brain is closely associated with numerous neurodegenerative diseases, including chronic pathologies such as Parkinson's,[1] Alzheimer's,[2] Huntington's,[3] headaches,[4] as well as neuronal damage in stroke.[5] Inhibition of nNOS, therefore, has become a compelling strategy for the treatment of neurodegeneration.[6–8] In the past two decades, a large number of nNOS inhibitors have been reported, including derivatives of L-arginines, guanidines, isothioureas, isothioureidos, 2-iminopiperidines, amidines, aminopyridines, thioureas, thiazoles, imidazoles, and indazoles.[9] None of these inhibitors, however, has entered clinical trials due to drawbacks with respect to their potency and isozyme selectivity.[9] These inhibitors, when binding to nNOS, target the L-arginine binding pocket where nNOS has high sequence homology with the other two isozymes, eNOS and iNOS.[6] This explains why most inhibitors suffer from poor isoform selectivity. At present, discovery of nNOS inhibitors with high potency and selectivity still represents a major challenge.

To overcome this limitation, a number of selective nNOS inhibitors have emerged from structure-based design.[10–12] One of the more important is pyrrolidine-based inhibitor **1**, which exhibits excellent potency (K_i = 7 nM) and selectivity for rat nNOS over bovine eNOS (2700-fold) and murine macrophage iNOS (830-fold).[13–15] Interestingly, crystal structures of nNOS and eNOS in complex with **1** revealed that this inhibitor adopts an unexpected 'flipped' binding mode, shown in Figure 1, in which the 2-amino-4-methylpyridine motif extended beyond the edge of the heme distal site, hydrogen bonded to the heme propionate of pyrrole ring D, and fits nicely into a hydrophobic pocket (Tyr^{706}, Leu^{337}, and Met^{336}) formed by an alternate rotamer of the aromatic side chain of Tyr^{706}.[13] A close look at this pocket indicates two potential beneficial interactions: (1) the hydrophobic interaction between the 4-methyl group of **1** and the side chains of Leu^{337} and Met^{336}, and (2) the π–π stacking interaction between the aminopyridine motif of **1** and the aromatic side chain of Tyr^{706}. More importantly, the specific residues around this pocket are significantly different in the three mammalian NOS isoforms. For example, instead of the three amino acid residues, Tyr^{706}, Leu^{337}, and Met^{336} for rat nNOS, for human nNOS the corresponding residues are Tyr^{710}, His^{341}, and Met^{340}, while for bovine eNOS and murine iNOS, these are Tyr^{477},

* Corresponding authors. Tel.: +1 949 824 7020 (T.L.P.); tel.: +1 847 491 5653 (R.B.S.).
E-mail addresses: poulos@uci.edu (T.L. Poulos), Agman@chem.northwestern.edu, r-silverman@northwestern.edu (R.B. Silverman).
† Present Address: Department of Chemistry, University of Louisiana at Lafayette, PO Box 44370, Lafayette, LA 70504, USA.
‡ Department of Pediatrics and Center for Applied Genomics, 1st School of Medicine, Charles University, Prague, Czech Republic.

0960-894X/$ - see front matter © 2010 Elsevier Ltd. All rights reserved.
doi:10.1016/j.bmcl.2010.08.096

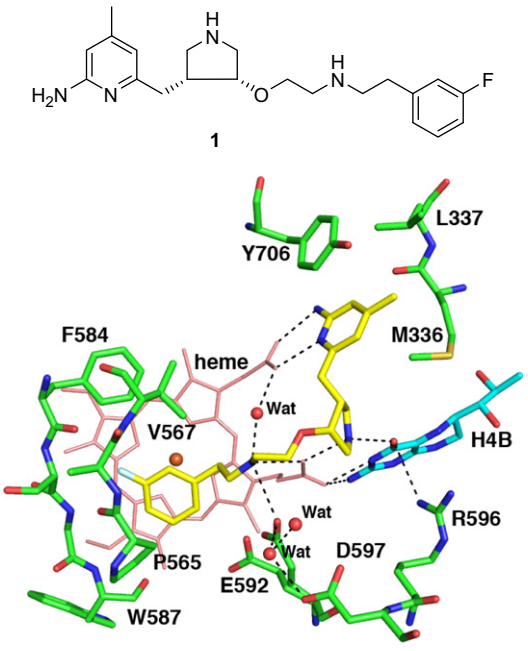

Figure 1. Binding of lead compound **1** to the rat nNOS active site. The major hydrogen bonds are drawn as dashed lines. The structural figures were prepared with PyMOL (www.pymol.org).

Leu[107], and Val[106], and Tyr[487], Asn[115], and Met[114], respectively.[16] Therefore, we speculate that this hydrophobic pocket may provide a new 'hot spot' for developing isoform-selective inhibitors for NOSs.

To further investigate the chemical environment of this peripheral site, and also to evaluate the possibility of utilizing it for the development of selective nNOS inhibitors, we report herein the synthesis and evaluation of three inhibitors, **2a**, **2b**, and **3**. Compound **2a** is an analog of **1**, with the 4-methyl group removed from the 2-aminopyridine ring. The difference in potency between **1** and **2a** for nNOS can demonstrate the importance of the methyl group to inhibitory activity. Compound **2b**, the enantiomer of **2a**, has opposite chirality at the pyrrolidine core. Therefore, **2b** cannot adopt the 'flipped' binding mode as with **2a**, and thus will provide a direct comparison between the two different binding modes. Inhibitor **3** removes the aromaticity of the aminopyridine from **2a**. A comparison of **3** and **2a** demonstrates the role of the π–π stacking interaction between the pyridine ring of **1** and the side chain of Tyr[706].

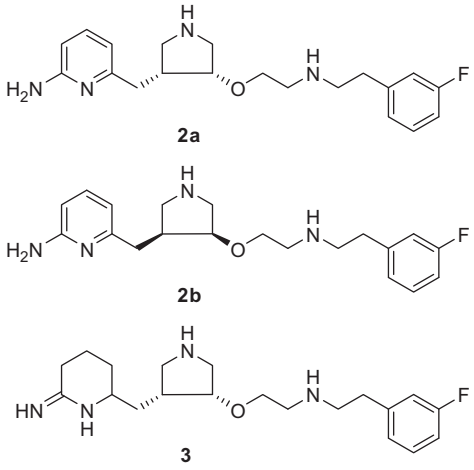

The syntheses of key intermediates **4a** and **4b** are shown in Scheme 1, using a recently reported method.[13–15] The amino group of 2-amino-4,6-dimethylpyridine (**5**) was protected using $(Boc)_2O$ in the presence of triethylamine (TEA) to provide **6** in high yields. Compound **6** was treated with two equivalents of *n*-BuLi, and the resulting dianion was allowed to react with the epoxide (**7**)[13] to generate the desired regioisomer (**8**) in modest yields. Then, the free NH group on the pyridine ring was further protected by a benzyl-protecting group using benzyl bromide to yield **9** in good yields. Next, *trans* alcohol **9** underwent a Mitsunobu reaction using acetic acid as a nucleophile to produce **10** in very high yields. Hydrolysis of **10** yielded *cis*-alcohol **11** in quantitative yields. Finally, the racemic mixture of **11** was successfully separated using a two step procedure. First, **11** was treated with (1*S*)-(−)-camphanic

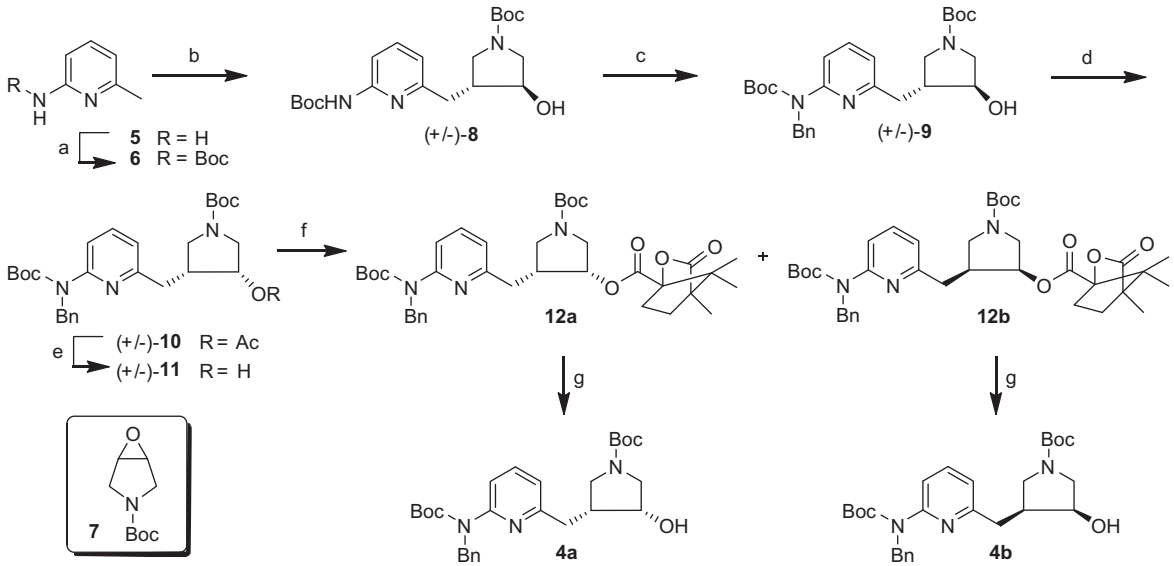

Scheme 1. Synthesis of **4a** and **4b**. Reagents and conditions: (a) $(Boc)_2O$, TEA, *t*-BuOH, 50 °C, 24 h, 90%; (b) (i) *n*-BuLi (2 equiv), −78 °C to rt, 30 min; (ii) **7**, −78 °C to rt, 3 h, 55%; (c) NaH, 0 °C to rt, 10 min, benzyl bromide, rt, 8 h, 92%; (d) PPh_3, DIAD, acetic acid, rt, 12 h, 95%; (e) NaOH (2 N)/MeOH, 50 °C, 4 h, 90%; (f) (1*S*)-(−)-camphanic chloride, TEA, DMAP, rt 4 h, 49% for each diastereomer; (g) Na_2CO_3, H_2O/MeOH, rt, 3 h, 99%.

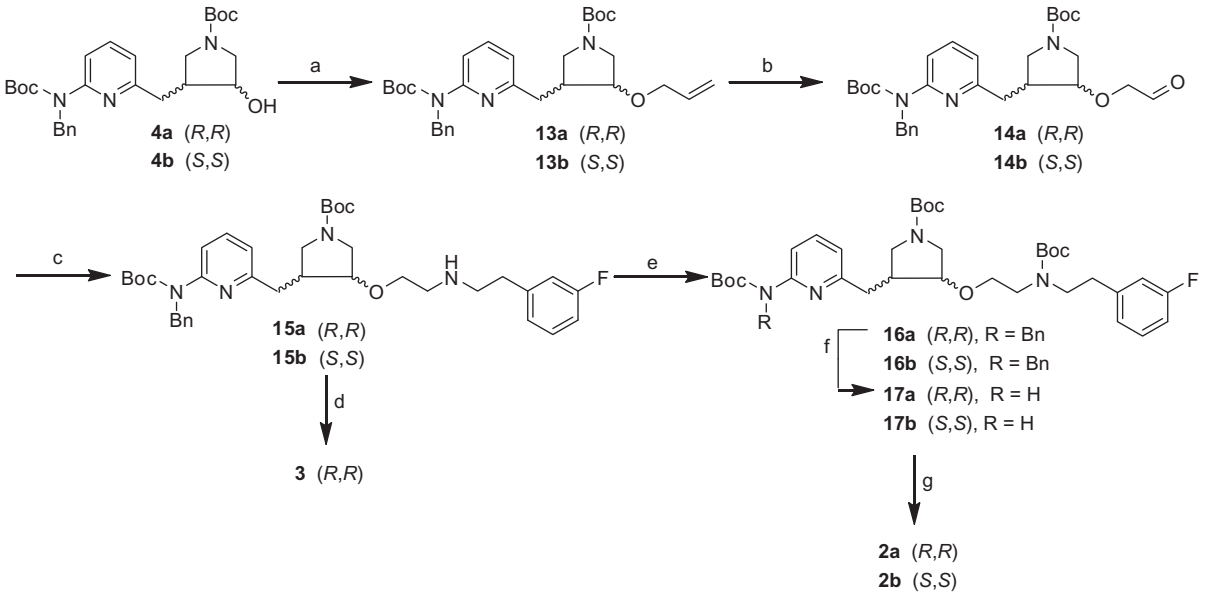

Scheme 2. Syntheses of **2a**, **2b**, and **3**. Reagents and conditions: (a) NaH, allyl bromide, 0 °C to rt 30 min, 99%; (b) (i) O_3, −78 °C; (ii) Zn, acetic acid, −78 °C to rt, 70–75%; (c) 2-(3-fluorophenyl)ethanamine, $NaHB(OAc)_3$, rt, 3 h, 52–55%; (d) $Pd(OH)_2/C$, H_2, 2:1 EtOH/HCl (12 N), rt, 575 psi, 40 h, 100%; (e) $(Boc)_2O$, Et_3N, MeOH, rt, 0.5 h, 99%; (f) $Pd(OH)_2/C$, H_2, 60 °C, 24 h, 35–50%; (g) 6 N HCl/MeOH (2:1), rt, 4 h, 80–85%.

chloride in the presence of TEA and *N*,*N*-dimethylaminopyridine (DMAP) to yield two diastereomers (**12a** and **12b**), which were successfully separated using silica chromatography. Then, each ester was subjected to aqueous Na_2CO_3 to produce **4a** and **4b** as single enantiomers in excellent yields.

Next, allylation of **4a**/**b** gave **13a**/**b** in excellent yields (Scheme 2).[13–15] Alkenes **13a**/**b** were subjected to ozonolysis using Zn as the reducing reagent to provide aldehydes (**14a**/**b**), which underwent reductive aminations with 2-(3-fluorophenyl)ethanamine to provide secondary amines **15a**/**b**. The secondary amino group was protected with a Boc-protecting group, and then the benzyl-protecting groups of **16a**/**b** were removed by catalytic hydrogenation at 60 °C to give **17a**/**b**. Finally, the three Boc-protecting groups were removed in a 2:1 mixture of 6 N HCl and MeOH to generate inhibitors **2a** and **2b**. Inhibitor **3** can be synthesized from **15a** using high pressure catalytic hydrogenation conditions in very high yields.

In the crystal structure of the active site of rat nNOS, **2a** adopts the same binding mode as lead compound **1** (Fig. 2A). The aminopyridine motif extends to the same peripheral hydrophobic pocket containing Tyr^{706}, Leu^{337}, and Met^{336}, forming a charge–charge interaction with the heme propionate D, as well as a π–π stacking interaction with the aromatic side chain of Tyr^{706}. However, removal of the 4-methyl group from the 2-aminopyridine motif dramatically impaired the potency (sevenfold) of the inhibitor (**2a** vs **1**, Table 1). This result highlights the crucial role of the 4-methyl group for retaining the high inhibitory activity of **1** for rat nNOS. Importantly, the selectivity of **2a** for rat nNOS over bovine eNOS also dropped significantly (2.3-fold, Table 1). This was mainly the result of the lower sensitivity of eNOS to the presence of the 4-methyl group, only a threefold difference when comparing **2a** to **1**. This methyl group might make less favorable contacts with the smaller side chain of Val^{106} in eNOS. Inhibitor **2b**, the corresponding enantiomer of **2a**, adopts the normal binding mode with its 2-aminopyridine hydrogen bonded to the side chain of Glu^{592} (Fig. 2B), resulting in a fourfold lower potency for rat nNOS (**2b** vs **2a**, Table 1). However, eNOS has no preference for the two binding modes with **2b** and **2a** showing comparable affinities. Inhibitor **3**, with the 2-aminopyridine of **2a** reduced to a cyclic amidine, showed diminished potency for rat nNOS (**3** vs **2a**, Table 1). This re-

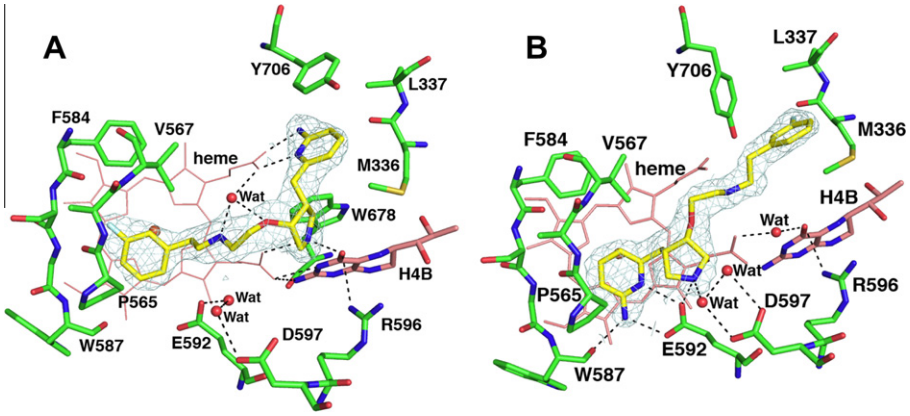

Figure 2. Active site structures of rat nNOS in complex with **2a** (A, PDB code 3NNY) and **2b** (B, PDB code 3NNZ). Shown also the 2Fo–Fc electron density for inhibitor at 1σ contour level. The major hydrogen bonds are drawn as dashed lines.

Table 1
K_i values of **1**, **2a**, **2b**, and **3** for rat nNOS, bovine eNOS and murine iNOS

Inhibitor	K_i[a] (nM)			Selectivity	
	Rat nNOS	eNOS	iNOS	n/e	n/i
1	7	19,000	5800	2700	830
2a	50	58,000	10,000	1200	200
2b	220	59,000	13,200	270	60
3	110	58,000	21,800	530	200

[a] The K_i values represent at least duplicate measurements with standard deviations of ±10%.

Table 2
K_i values of **1**, **2a**, **2b**, and **3** for rat nNOS and human nNOS

Inhibitor	K_i[a] (nM)		Selectivity
	Rat nNOS	Human nNOS	Rat/human
1	7	50	7.1
2a	50	290	5.8
2b	220	1800	8.2
3	110	490	4.5

[a] The K_i values represent at least duplicate measurements with standard deviations of ±10%.

sult indicates that the π–π stacking interaction between the pyridine ring and Tyr^{706} is an important factor for tight binding of **2a** to nNOS. The stacking interaction provides less contribution to the binding affinity of **2a** to eNOS, as its K_i values are similar for both **3** and **2a**. This is probably because the Tyr^{477} side chain in eNOS does not interact as closely with the 2-aminopyridine ring of the inhibitors, as demonstrated previously in crystal structures for other pyrrolidine inhibitors complexed to eNOS and nNOS.[13]

We also tested the inhibitory activity of **1**, **2a**, **2b**, and **3** against the human isoform of nNOS (Table 2). Human nNOS shows very high sequence homology to rat nNOS in the active site[16]; the only different residue in the peripheral site is His^{341} in place of Leu^{337}, which makes the hydrophobic pocket in human nNOS smaller than that in rat nNOS. As a result, the hydrophobic pocket of human nNOS should prefer smaller fragments. Even though inhibitors **1**, **2a**, **2b**, and **3** are less potent with human nNOS compared to rat nNOS, the selectivity ($K_{i\text{-human}}/K_{i\text{-rat}}$) dropped 1.2-fold and 1.6-fold for **2a** and **3**, respectively, compared to **1**. These results indicate that the relatively smaller hydrophobic pocket in human nNOS prefers to bind the non-substituted aminopyridine fragment.

In summary, we demonstrate the feasibility and potential of using the peripheral site (Tyr^{706}, Leu^{337}, and Met^{336} for rat nNOS) as a 'hot spot' for designing potent and selective nNOS inhibitors. Three new inhibitors, **2a**, **2b**, and **3**, have been synthesized. The crystal structures show that **2a** shares the same flipped binding mode as lead compound **1**, while **2b** binds in a normal mode as expected by their stereochemistry of the pyrrolidine ring. The inhibitory activities were tested against various NOS isoforms. Our results highlight the importance of the hydrophobic interaction between the 4-methyl group of the 2-aminopyridine motif and the side chain of Met^{336} for tight binding and high isoform-selectivity of the inhibitors. We also show that the π–π stacking interaction between the aminopyridine ring and the aromatic side chain of Tyr^{706} is important for good potency. The insensitivity of eNOS to the binding mode of pyrrolidine-based inhibitors and the weaker π–π stacking interaction from its Tyr^{477} to the 2-aminopyridine ring of the inhibitors are isoform specific properties valuable to future inhibitor design.

Acknowledgments

The authors are grateful to the National Institutes of Health for financial support to R.B.S. (GM49725), T.L.P. (GM57353), and Dr. Bettie Sue Masters (GM52419, with whose laboratory P.M. and L.J.R. are affiliated). B.S.S.M. is the Robert A. Welch Distinguished Professor in Chemistry (AQ0012). P.M. is supported by Grants 0021620806 and 1M0520 from MSMT of the Czech Republic.

Supplementary data

Supplementary data associated with this article can be found in the online version at doi:10.1016/j.bmcl.2010.08.096.

References and notes

1. Zhang, L.; Dawson, V. L.; Dawson, T. M. *Pharmacol. Ther.* **2006**, *109*, 33.
2. Dorheim, M.-A.; Tracey, W. R.; Pollock, J. S.; Grammas, P. *Biochem. Biophys. Res. Commun.* **1994**, *205*, 659.
3. Norris, P. J.; Waldvogel, H. J.; Faull, R. L. M.; Love, D. R.; Emson, P. C. *Neuronsicence* **1996**, *72*, 1037.
4. Ashina, M. *Exp. Opin. Pharmacother.* **2002**, *3*, 395.
5. Sims, N. R.; Anderson, M. F. *Neurochem. Int.* **2002**, *40*, 511.
6. Alderton, W. K.; Cooper, C. E.; Knowles, R. G. *Biochem. J.* **2001**, *357*, 593.
7. Southan, G. J.; Szabo, C. *Biochem. Pharmacol.* **1996**, *51*, 383.
8. Babu, B. R.; Griffith, O. W. *Curr. Opin. Chem. Biol.* **1998**, *2*, 491.
9. Ji, H.; Erdal, E. P.; Litzinger, E. A.; Seo, J.; Zhu, Y.; Xue, F.; Fang, J.; Huang, J.; Silverman, R. B.. In *Frontiers in Medicinal Chemistry*; Reitz, A. B., Choudhary, M. I., Atta-ur-Rahman, Eds.; Bentham Science, 2009; Vol. 54, p 842.
10. Silverman, R. B. *Acc. Chem. Res.* **2009**, *42*, 439.
11. Fedorov, R.; Vasan, R.; Ghosh, D. K.; Schlichting, I. *Proc. Natl. Acad. Sci. U.S.A.* **2004**, *101*, 5892.
12. Garcin, E. D.; Arvai, A. S.; Rosenfeld, R. J.; Kroeger, M. D.; Crane, B. R.; Andersson, G.; Andrews, G.; Hamley, P. J.; Mallinder, P. R.; Nicholls, D. J.; St-Gallay, S. A.; Tinker, A. C.; Gensmantel, N. P.; Mete, A.; Cheshire, D. R.; Connolly, S.; Stuehr, D. J.; Aberg, A.; Wallace, A. V.; Tainer, J. A.; Getzoff, E. D. *Nat. Chem. Biol.* **2008**, *4*, 700.
13. (a) Delker, D. L.; Ji, H.; Li, H.; Jamal, J.; Fang, J.; Xue, F.; Silverman, R. B.; Poulos, T. L. *J. Am. Chem. Soc* **2010**, *132*, 5437; (b) Ji, H.; Delker, S. L.; Li, H.; Martásek, P.; Roman, L. J.; Poulos, T.P.; Silverman, R. B. *J. Med. Chem.*, in press.
14. Lawton, G. R.; Ranaivo, H. R.; Wing, L. K.; Ji, H.; Xue, F.; Martesek, P.; Roman, L. J.; Watterson, D. M. *Bioorg. Med. Chem.* **2009**, *17*, 2371.
15. Xue, F.; Fang, J.; Lewis, W. W.; Martasek, P.; Roman, L. J.; Silverman, R. B. *Bioorg. Med. Chem. Lett.* **2010**, *20*, 554.
16. Ji, H.; Li, H.; Flinspach, M.; Poulos, T. L.; Silverman, R. B. *J. Med. Chem.* **2003**, *46*, 5700.